

Weakly-supervised Multi-output Regression via Correlated Gaussian Processes

Seokhyun Chung¹ Raed Al Kontar¹ Zhenke Wu²

Abstract

Multi-output regression seeks to infer multiple latent functions using data from multiple groups/sources while accounting for potential between-group similarities. In this paper, we consider multi-output regression under a weakly-supervised setting where a subset of data points from multiple groups are unlabeled. We use dependent Gaussian processes for multiple outputs constructed by convolutions with shared latent processes. We introduce hyperpriors for the multinomial probabilities of the unobserved labels and optimize the hyperparameters which we show improves estimation. We derive two variational bounds: (i) a modified variational bound for fast and stable convergence in model inference, (ii) a scalable variational bound that is amenable to stochastic optimization. We use experiments on synthetic and real-world data to show that the proposed model outperforms state-of-the-art models with more accurate estimation of multiple latent functions and unobserved labels.

1. Introduction

The goal of multi-output regression is to estimate multiple latent functions, each corresponding to a group or a source, over a common domain of input and output. It learns from the observed input, output and source membership label $\{(x_i, y_i, z_i)\}$ by borrowing strength from potential between-source commonalities. The capability to account for dependencies between outputs improves the accuracy of prediction and estimation. Indeed, in recent years, multi-output regression has seen great success within the machine learning community, specifically in Gaussian processes (GP) (e.g., Dai et al., 2017; Álvarez & Lawrence, 2011). This success is mainly attributed to the fact that correlated outputs can be expressed as a realization from

¹Department of Industrial & Operations Engineering, University of Michigan, Ann Arbor, Michigan, USA ²Department of Biostatistics, University of Michigan, Ann Arbor, Michigan, USA. Correspondence to: Raed Al Kontar <alkontar@umich.edu>.

a single GP, where commonalities are modeled through inducing cross-correlations between outputs (e.g., Álvarez et al., 2013; Kaiser et al., 2018a; Kontar et al., 2018). In the literature, the resulting GP has been termed “Multi-output”, “Multivariate” or a “Multi-task” GP. In this paper we refer to this class of models as MGP.

However, the success stories of MGPs have mainly relied on the existence of *fully labeled data*, where for each observation there exists a correct label that indicates its group membership. In many applications, group labels are often hard or expensive to obtain, creating acute needs for methods that can handle data without complete group labels. We first illustrate the hypothetical scenario in Figure 1. Con-

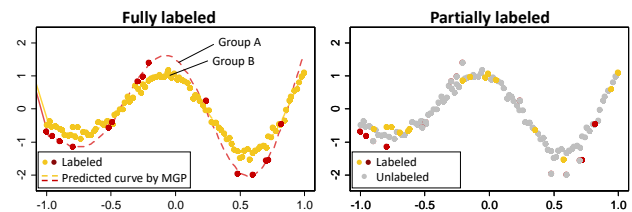


Figure 1. Examples of fully labeled (left) and partially labeled (right) settings for multi-output regression.

sider a regular physical examination that assesses diabetic risk through measuring an individual’s blood glucose level and body mass index (BMI) for two groups: AIDS (group A) and non-AIDS individuals (group B). On the one hand, we may expect sparse observations in group A compared to group B if the AIDS prevalence is low in the population being examined. Modeling the blood-glucose-level-versus-BMI curves independently *a priori* for the two groups will result in unstable predictions for group A with fewer observations. This can be addressed by using an MGP which borrows information from the densely observed group B to inform group A. On the other hand, the output labels are not always fully available. For example, due to privacy concerns, some AIDS patients may choose not to report their AIDS status; A subset of non-AIDS patients may also not report the AIDS status. This results in data points with unobserved labels for a subset of subjects in both groups (see Figure 1, Right). This aspect presents a critical challenge for the use of MGPs in such scenarios.

In this paper, we address this key challenge through an MGP-based probabilistic model that can jointly infer the

group labels and the underlying latent functions for all the groups. We refer to our model as weakly-supervised regression (Zhou, 2017) because it can handle (i) unlabeled data (i.e., semi-supervised setting), (ii) noisy labels, (iii) prior belief on group memberships. Specifically, the membership for each data point is assumed to follow a multinomial distribution. For the labeled data points, this allows prior belief on label memberships to be included. For the unlabeled observations, we assign a Dirichlet prior on the multinomial probabilities. *The Dirichlet prior acts as a regularizer that controls group assignment acuteness and in turn is capable of minimizing predictive variance.* Correlation between the outputs are then induced through sparse convolution processes with a layer of shared latent processes, which are amenable to computationally efficient posterior inferential algorithms via sparse approximations. We then show how the sparse model seamlessly integrates the label prior probabilities. To overcome posterior intractability we derive a variational bound and show that it interestingly turns out to have similar structure to a typical MGP. Using the structural similarity, a scalable variational bound amenable to stochastic optimization is obtained.

In the following, we summarize the major contributions of this paper.

1. We introduce a weakly-supervised regression framework based on correlated GPs that efficiently learns missing labels and estimates conditional means and variances for multiple groups. The model leverages unlabeled data to improve performance over a range of weakly-supervised settings including semi-supervision, noisy labels and prior belief on group memberships. To the best of our knowledge, this is the first study that addresses the weakly-supervised setting in MGP. We remark that in our model we exploit the popular convolved GPs (Álvarez & Lawrence, 2011) to establish cross dependencies, however, our framework is applicable to any separable or non-separable GP construction.
2. We derive two variational bounds. First, we derive a modified variational lower bound for the marginal likelihood. The modified bound enjoys (i) interpretability which allows us to obtain some useful insights of the proposed model, (ii) ease of modeling whereby any MGP construction can be plugged into the lower bound, and (iii) stability due to faster convergence. The bound indeed shares a close structure to a fully labeled MGP, and inspired from this, we derive an alternative scalable variational bound that stochastic optimization methods can be used to maximize.
3. We provide a mechanism to control assignment acuteness of unlabeled data via a Dirichlet prior on the multinomial probabilities. We highlight the analytical properties of this mechanism, specifically compared to state-of-the-art data association methods in GPs (Lázaro-Gredilla et al., 2012) which face the challenge of acute label assignment (see Sec-

tion 4.3) resulting in high predictive variance and obscure assignments.

4. We illustrate the model and inferential algorithm using two challenging datasets: housing price index and climate data. We show that our model can leverage unlabeled data to improve predictive performance and reliably recover unobserved or noisy labels.

2. Background

2.1. Multioutput GPs: Fully-Labeled

Consider a dataset with N observations, $\mathcal{D} = \{\mathbf{X}, \mathbf{y}\}$ where $\mathbf{X} \in \mathbb{R}^{N \times d}$ and $\mathbf{y} \in \mathbb{R}^{N \times 1}$ are the inputs and outputs, respectively; Each observation is drawn from one of M groups. Now, suppose we observe the group labels $h_n \in \{1, \dots, M\}$, for observation $n = 1, \dots, N$. Let N_m represent the number of observations from output m ; We have $N = \sum_{m=1}^M N_m$. Without loss of generality, we re-order the rows in \mathcal{D} by the ascending order of the group labels $\{h_n\}$. That is, we write \mathbf{y} and \mathbf{X} as: $\mathbf{y} = [\mathbf{y}_1^T, \dots, \mathbf{y}_M^T]^T$ with corresponding inputs $\mathbf{X} = [\mathbf{X}_1^T, \dots, \mathbf{X}_M^T]^T$ where $\mathbf{y}_m = [y_{1m}, \dots, y_{N_m m}]^T$, $\mathbf{X}_m = [\mathbf{x}_{1m}^T, \dots, \mathbf{x}_{N_m m}^T]^T$ and $\mathbf{x}_{nm} \in \mathbb{R}^{1 \times d}$ for $m \in \{1, \dots, M\}$.

Given a source $m = 1, \dots, M$, we assume the vector of outputs obtained at distinct input values follows $y_{nm} = f_m(\mathbf{x}_{nm}) + \epsilon_{nm}$, for observation $n = 1, \dots, N_m$, where $f_m(\cdot)$ and $\epsilon_{nm} \sim \mathcal{N}(0, \sigma_m^2)$ denote the m -th unknown regression function and an independent additive Gaussian noise, respectively. Assuming Gaussian process priors for $\{f_m(\cdot)\}$, the exact MGP likelihood upon integrating over $f_m(\cdot)$ is given as $p(\mathbf{y}|\mathbf{X}, \phi) = \mathcal{N}(\mathbf{0}, \mathbf{K} + \mathbf{\Sigma})$, where $\mathbf{K} \in \mathbb{R}^{N \times N}$ is an arbitrary covariance matrix. Here ϕ are hyperparameters for \mathbf{K} , an M by M block matrix; \mathbf{K} is comprised of block covariance (on the main diagonal blocks) and cross-covariance (off-diagonal blocks) matrices. The (m, m') -th block $\mathbf{K}_{\mathbf{f}_m, \mathbf{f}_{m'}}$ is of dimension $N_m \times N_{m'}$ with elements $k_{f_m, f_{m'}}(\mathbf{x}, \mathbf{x}') = \text{cov}(f_m(\mathbf{x}), f_{m'}(\mathbf{x}'))$, for any \mathbf{x} and \mathbf{x}' from group m and m' , respectively; $\mathbf{\Sigma} = \text{bdiag}(\sigma_m^2 \mathbf{I}_{N_m})_{m=1}^M$ where the notation $\text{bdiag}(\mathbf{G}_m)_{m=1}^M$ indicates a block diagonal matrix with $\mathbf{G}_1, \dots, \mathbf{G}_M$ on the main diagonal.

2.2. Sparse Convolved MGP (SCMGP)

To induce cross-correlations between the latent functions (off-diagonal blocks in \mathbf{K}), we use convolved MGPs. For example, the class of separable covariances or the linear model of coregionalization are special cases of the convolution construction (Álvarez et al., 2012; Fricker et al., 2013). Convolved MGPs build the covariance matrix \mathbf{K} via $f_m(\mathbf{x}) = \int_{-\infty}^{\infty} k_m(\mathbf{x} - \mathbf{w})u(\mathbf{w})d\mathbf{w}$, $m = 1, \dots, M$, where $k_m(\mathbf{x})$ denotes a smoothing kernel and $u(\mathbf{w})$ is a shared latent GP. The key rationale is to share the common

latent GP $u(\cdot)$ across M sources. Since convolution is a linear operator, the outputs \mathbf{y} are then samples from multiple interrelated GPs - an MGP. This construction readily generalizes to multiple shared latent GPs. We refer readers to [Álvarez et al. \(2012\)](#) for further details.

The key advantage of convolved MGPs is that they are amenable to sparse approximations in a similar fashion as in univariate GPs ([Quiñonero-Candela & Rasmussen, 2005](#)). This is done through approximating \mathbf{K} using conditional independence assumptions. The approximation is built from a sparse set of inducing points (length $Q \ll N$) $\mathbf{u} = [u(\mathbf{w}_1), \dots, u(\mathbf{w}_Q)]^T$ where given \mathbf{u} , $f_1(\mathbf{x}), \dots, f_M(\mathbf{x})$ are *a priori* conditionally independent. This can be written as $p(\mathbf{y}|\mathbf{u}, \mathbf{W}, \mathbf{X}, \boldsymbol{\theta}) = \prod_{m=1}^M p(\mathbf{y}_m|\mathbf{u}, \mathbf{W}, \mathbf{X}_m, \boldsymbol{\theta}) = \mathcal{N}(\mathbf{y}|\mathbf{K}_{\mathbf{f},\mathbf{u}}\mathbf{K}_{\mathbf{u},\mathbf{u}}^{-1}\mathbf{u}, \mathbf{B} + \boldsymbol{\Sigma})$, where $\mathbf{W} = \{\mathbf{w}_q\}_{q=1}^Q$; $p(\mathbf{u}|\mathbf{W}) = \mathcal{N}(\mathbf{u}|\mathbf{0}, \mathbf{K}_{\mathbf{u},\mathbf{u}})$; $\mathbf{K}_{\mathbf{f},\mathbf{u}} = \mathbf{K}_{\mathbf{u},\mathbf{f}}^T$ is a cross-covariance matrix relating the column vector $\mathbf{f} = [\mathbf{f}_1^T, \dots, \mathbf{f}_M^T]^T$ and \mathbf{u} where the column vector $\mathbf{f}_m = f_m(\mathbf{X}_m) = [f_m(\mathbf{x}_{1m}), \dots, f_m(\mathbf{x}_{N_m m})]^T$ collects f_m values at each of N_m inputs in group m . Additionally, $\mathbf{B} = \text{bdiag}(\mathbf{B}_m)_{m=1}^M$ with $\mathbf{B}_m = \mathbf{K}_{\mathbf{f}_m, \mathbf{f}_m} - \mathbf{K}_{\mathbf{f}_m, \mathbf{u}}\mathbf{K}_{\mathbf{u}, \mathbf{u}}^{-1}\mathbf{K}_{\mathbf{u}, \mathbf{f}_m}$, where $\mathbf{K}_{\mathbf{f}_m, \mathbf{f}_m}$ is a covariance matrix of \mathbf{f}_m ; $\mathbf{K}_{\mathbf{f}_m, \mathbf{u}} = \mathbf{K}_{\mathbf{u}, \mathbf{f}_m}^T$ is a cross-covariance matrix between \mathbf{f}_m and \mathbf{u} ; $\boldsymbol{\theta}$ is a set of hyperparameters. The marginal likelihood is:

$$\begin{aligned} p(\mathbf{y}|\mathbf{W}, \mathbf{X}, \boldsymbol{\theta}) &= \int p(\mathbf{y}|\mathbf{u}, \mathbf{W}, \mathbf{X}, \boldsymbol{\theta})p(\mathbf{u}|\mathbf{W})d\mathbf{u} \\ &= \mathcal{N}(\mathbf{y}|\mathbf{0}, \mathbf{B} + \mathbf{K}_{\mathbf{f},\mathbf{u}}\mathbf{K}_{\mathbf{u},\mathbf{u}}^{-1}\mathbf{K}_{\mathbf{u},\mathbf{f}} + \boldsymbol{\Sigma}). \end{aligned} \quad (1)$$

Notice that we only introduce one latent process, but it is easy to generalize for multiple latent processes. As shown in Eq. (1), the key idea is approximating \mathbf{K} by $\mathbf{B} + \mathbf{K}_{\mathbf{f},\mathbf{u}}\mathbf{K}_{\mathbf{u},\mathbf{u}}^{-1}\mathbf{K}_{\mathbf{u},\mathbf{f}}$ which is equal to the \mathbf{K} in the block diagonals and a low rank approximation in the off-diagonal blocks. Indeed, such approximation is derived from variational inference where the recent work of [Burt et al. \(2019\)](#) provided a theoretical foundation for such approximations showing that the variational bound can made arbitrarily small to the exact GP with $Q \ll N$ ($Q = \mathcal{O}(\log^d(N))$ for the exponential kernel).

3. Weakly-Supervised MGP

Now we discuss our model, referred to as weakly-supervised MGP (WSMGP). We first present the general probabilistic framework, and then utilize SCMGP in the framework. We use superscripts l and u to indicate quantities associated with “labeled” and “unlabeled” observations, respectively.

Unlike the fully-labeled MGP, we now have $N = N^u + N^l$ observations comprised of N^u unlabeled $\{(\mathbf{x}_i^u, y_i^u)\}_{i=1, \dots, N^u}$ and N^l labeled observations $\{(\mathbf{x}_i^l, y_i^l)\}_{i=1, \dots, N^l}$. For each labeled observation, we have a

vector of labels $\mathbf{h} = [h_n]_{n=1, \dots, N^l}^T$ where $h_n \in \{1, \dots, M\}$ specifies that the n -th observation originates from the h_n -th group.

For the n -th labeled observation we introduce a vector of unknown binary indicators $\mathbf{z}_n^l = (z_{nm}^l)_{m=1, \dots, M}^T$, where $\sum_{m=1}^M z_{nm}^l = 1$ and $z_{nm}^l \in \{0, 1\}$. Let $z_{nm}^l = 1$ indicate that the latent function $f_m(\cdot)$ generated observation n . We define $\mathbf{z}_n^u = (z_{nm}^u)_{m=1, \dots, M}^T$ similarly defined for the unlabeled observations.

For notational clarity, we collectively define additional notations as follows: the inputs $\mathbf{X}^u = [\mathbf{x}_n^u]_{n=1, \dots, N^u}^T$, $\mathbf{X}^l = [\mathbf{x}_n^l]_{n=1, \dots, N^l}^T$, $\mathbf{X} = [(\mathbf{X}^u)^T, (\mathbf{X}^l)^T]^T$, the observed responses $\mathbf{y}^u = (y_n^u)_{n=1, \dots, N^u}^T$, $\mathbf{y}^l = (y_n^l)_{n=1, \dots, N^l}^T$, $\mathbf{y} = [(\mathbf{y}^u)^T, (\mathbf{y}^l)^T]^T$, the group indicators $\mathbf{Z}^u = [\mathbf{z}_n^u]_{n=1, \dots, N^u}^T$, $\mathbf{Z}^l = [\mathbf{z}_n^l]_{n=1, \dots, N^l}^T$, $\mathbf{Z} = [(\mathbf{Z}^u)^T, (\mathbf{Z}^l)^T]^T$, the noise levels $\boldsymbol{\sigma} = [\sigma_m]_{m=1, \dots, M}^T$ and the unknown functions \mathbf{f} .

Our model can then be formulated as follows:

$$p(\mathbf{y}|\mathbf{f}, \mathbf{Z}, \boldsymbol{\sigma}) = \prod_{n,m=1}^{N,M} \mathcal{N}([y]_n | [\mathbf{f}_m]_n, \sigma_m^2)^{[\mathbf{Z}]_{nm}}, \quad (2)$$

$$p(\mathbf{f}|\mathbf{X}, \boldsymbol{\phi}) = \mathcal{N}(\mathbf{f}|\mathbf{0}, \mathbf{K}), \quad (3)$$

$$\begin{aligned} p(\mathbf{Z}|\boldsymbol{\Pi}) &= \prod_{n,m=1}^{N,M} [\boldsymbol{\Pi}]_{nm}^{[\mathbf{Z}]_{nm}} = p(\mathbf{Z}^u|\boldsymbol{\Pi}^u)p(\mathbf{Z}^l|\boldsymbol{\Pi}^l) \\ &= \prod_{n,m=1}^{N^u,M} [\boldsymbol{\Pi}^u]_{nm}^{[\mathbf{Z}]_{nm}} \prod_{n,m=1}^{N^l,M} [\boldsymbol{\Pi}^l]_{nm}^{[\mathbf{Z}]_{nm}}, \end{aligned} \quad (4)$$

where \mathbf{Z} *a priori* follows independent multinomial distributions with parameters $\boldsymbol{\Pi} \in [0, 1]^{N \times M}$, where an element $[\boldsymbol{\Pi}]_{nm}$ indicates the probability that the observation n is generated from the source m ; Thus $\sum_{m=1}^M [\boldsymbol{\Pi}]_{nm} = 1$ for all $n \in \{1, \dots, N\}$. Here we have organized the probabilities by $\boldsymbol{\Pi} = [(\boldsymbol{\Pi}^u)^T, (\boldsymbol{\Pi}^l)^T]^T$ where $\boldsymbol{\Pi}^u = [(\boldsymbol{\pi}_n^u)^T]_{n=1, \dots, N^u}^T \in [0, 1]^{N^u \times M}$ and $\boldsymbol{\Pi}^l \in [0, 1]^{N^l \times M}$.

For each labeled observation $n = 1, \dots, N^l$, we give the probabilities $\boldsymbol{\Pi}^l$ specific values. The probabilities are determined by the level of uncertainty of the label h_n . For example, if we are perfectly sure about h_n , we can set $[\boldsymbol{\Pi}]_{nm} = \mathbb{I}(h_n = m)$, where $\mathbb{I}(A)$ is the indicator function and equals 1 if the statement A is true; 0 otherwise.

For each unlabeled observation $n = 1, \dots, N^u$, we place a Dirichlet prior on $\boldsymbol{\pi}_n^u$:

$$p(\boldsymbol{\pi}_n^u | \boldsymbol{\alpha}_0) = \text{Dir}(\boldsymbol{\pi}_n^u | \boldsymbol{\alpha}_0) = \frac{1}{\mathbf{B}(\boldsymbol{\alpha}_0)} \prod_{m=1}^M [\pi_n^u]_m^{\alpha_0 - 1}, \quad (5)$$

where $\mathbf{B}(\boldsymbol{\alpha}_0) = \frac{M\Gamma(\boldsymbol{\alpha}_0)}{\Gamma(M\boldsymbol{\alpha}_0)}$, a multivariate Beta function with parameter $\boldsymbol{\alpha}_0 = (\alpha_0)_{m=1, \dots, M}$. In general, the elements of

α_0 need not be identical; In this paper, for simplicity, we use identical α_0 for all the elements, i.e., symmetric Dirichlet. Hereon, we omit the hyperparameters $\{\theta, \sigma, \mathbf{h}, \alpha_0\}$ from the probabilistic models.

Apply SCMGP in Our Framework In Eq. (3) we modeled \mathbf{f} as an MGP with a full covariance matrix \mathbf{K} . In this paper, we use SCMGP as a sparse approximation to the full covariance. That is, we replace the full MGP (3) by

$$p(\mathbf{f}|\mathbf{u}, \mathbf{X}, \mathbf{W}) = \mathcal{N}(\mathbf{f}|\mathbf{K}_{\mathbf{f},\mathbf{u}}\mathbf{K}_{\mathbf{u},\mathbf{u}}^{-1}\mathbf{u}, \mathbf{B}), \quad (6)$$

$$p(\mathbf{u}|\mathbf{W}) = \mathcal{N}(\mathbf{u}|\mathbf{0}, \mathbf{K}_{\mathbf{u},\mathbf{u}}). \quad (7)$$

Our framework is not restricted to the SCMGP, because any approximation of \mathbf{K} can be utilized. Nevertheless, we use SCMGP in this paper for its computational efficiency, generality and fast convergence rates. Based on the probability distributions (2)-(7), the marginal log-likelihood is

$$\log p(\mathbf{y}|\mathbf{X}, \mathbf{W}) = \log \int_{\mathbf{f}, \mathbf{u}, \mathbf{Z}, \mathbf{\Pi}^u} \left(p(\mathbf{y}|\mathbf{f}, \mathbf{Z}) p(\mathbf{f}|\mathbf{u}, \mathbf{X}, \mathbf{W}) p(\mathbf{u}|\mathbf{W}) p(\mathbf{Z}|\mathbf{\Pi}) p(\mathbf{\Pi}^u) \right), \quad (8)$$

where $\int_{\mathbf{a}}(\cdot)$ represents integration over the ranges of variables in \mathbf{a} .

4. Inference

Derivation of the posterior distribution of WSMGP, $p(\mathbf{f}, \mathbf{u}, \mathbf{Z}, \mathbf{\Pi}|\mathbf{X}, \mathbf{y})$, is analytically intractable. A popular technique addressing this challenge is variational inference (VI) (Blei et al., 2017). VI approximates the posterior distribution maximizing a evidence lower bound (ELBO) on the marginal likelihood which is equivalent to minimizing the Kullback-Leibler (KL) divergence $\text{KL}(q(\mathbf{f}, \mathbf{u}, \mathbf{Z}, \mathbf{\Pi})||p(\mathbf{f}, \mathbf{u}, \mathbf{Z}, \mathbf{\Pi}|\mathbf{X}, \mathbf{y}))$ between the candidate variational distributions q and the true posterior.

Here we note that in GPs, traditional VI uses a mean-field approximation which assumes that the latent variables in variational distributions are independent, i.e., $q(\mathbf{f}, \mathbf{u}, \mathbf{Z}, \mathbf{\Pi}) = q(\mathbf{f})q(\mathbf{u})q(\mathbf{Z})q(\mathbf{\Pi})$ (Titsias, 2009). This has been the basis of many recent extensions and application of Vi in literature (e.g., Zhao & Sun, 2016; Hensman et al., 2013; Panos et al., 2018). Hereon, the well-known ELBO derived by the mean-field approximation is denoted as \mathcal{L}_{VB} .

4.1. Variational Approximation with Improved Lower Bound

In our model, we derive an alternative bound based on the observation that the latent variables \mathbf{f} and \mathbf{u} can be analytically marginalized out from Eq. (8). Thus, we only introduce variational distributions over $q(\mathbf{Z})$ and $q(\mathbf{\Pi}^u)$ that belong to the same distributional families as those of the origi-

nal distributions $p(\mathbf{Z})$ and $p(\mathbf{\Pi}^u)$. We distinguish the variational parameters from original by using the hat notation (e.g., $\hat{\mathbf{\Pi}}$). We refer the new bound to as the KL-corrected variational bound \mathcal{L}_{cVB} . To derive \mathcal{L}_{cVB} , we first observe the following inequality: $\log \int_{\mathbf{Z}, \mathbf{\Pi}^u} p(\mathbf{y}|\mathbf{f}, \mathbf{Z}) p(\mathbf{Z}|\mathbf{\Pi}) p(\mathbf{\Pi}^u) \geq \int_{\mathbf{Z}, \mathbf{\Pi}^u} q(\mathbf{Z}) q(\mathbf{\Pi}^u) \log \frac{p(\mathbf{y}|\mathbf{f}, \mathbf{Z}) p(\mathbf{Z}|\mathbf{\Pi}) p(\mathbf{\Pi}^u)}{q(\mathbf{Z}) q(\mathbf{\Pi}^u)}$ as a direct application of Jensen's inequality. Exponentiating each side of the above inequality and plugging it into Eq. (8), we find

$$\mathcal{L}_{\text{cVB}} = \log \int_{\mathbf{f}, \mathbf{u}} \left(e^{\int_{\mathbf{Z}, \mathbf{\Pi}^u} q(\mathbf{Z}) q(\mathbf{\Pi}^u) \log \frac{p(\mathbf{y}|\mathbf{f}, \mathbf{Z}) p(\mathbf{Z}|\mathbf{\Pi}) p(\mathbf{\Pi}^u)}{q(\mathbf{Z}) q(\mathbf{\Pi}^u)}} p(\mathbf{f}|\mathbf{u}, \mathbf{X}, \mathbf{W}) p(\mathbf{u}|\mathbf{W}) \right) \leq \log p(\mathbf{y}|\mathbf{X}, \mathbf{W}).$$

Now we can analytically calculate the integral resulting in the following interpretable form

$$\mathcal{L}_{\text{cVB}} = \log \mathcal{N}(\mathbf{y}|\mathbf{0}, \mathbf{B} + \mathbf{K}_{\mathbf{f},\mathbf{u}}\mathbf{K}_{\mathbf{u},\mathbf{u}}^{-1}\mathbf{K}_{\mathbf{u},\mathbf{f}} + \mathbf{D}) + \mathcal{V}, \quad (9)$$

where $\mathbf{D} = \text{bdiag}(\mathbf{D}_m)_{m=1}^M$, \mathbf{D}_m is a diagonal matrix with elements $\sigma_m^2/[\hat{\mathbf{\Pi}}]_{1m}, \dots, \sigma_m^2/[\hat{\mathbf{\Pi}}]_{Nm}$ and

$$\begin{aligned} \mathcal{V} = & -\text{KL}(q(\mathbf{Z}^l)||p(\mathbf{Z}^l|\mathbf{\Pi}^l)) \\ & -\text{KL}(q(\mathbf{Z}^u)q(\mathbf{\Pi}^u)||p(\mathbf{Z}^u|\mathbf{\Pi}^u)p(\mathbf{\Pi}^u)) \\ & + \frac{1}{2} \sum_{n=1, m=1}^{N, M} \log \frac{(2\pi\sigma_m^2)^{(1-[\hat{\mathbf{\Pi}}]_{nm})}}{[\hat{\mathbf{\Pi}}]_{nm}}. \end{aligned}$$

A detailed derivation of Eq. (9) is provided in the supplementary materials. We maximize \mathcal{L}_{cVB} to obtain the optimizing variational parameters $\{\hat{\mathbf{\Pi}}, \hat{\alpha}\}$ and hyperparameters $\{\theta, \sigma\}$ as our estimates. Note that the computational complexity is dominated by the inversion of $\mathbf{B} + \mathbf{K}_{\mathbf{f},\mathbf{u}}\mathbf{K}_{\mathbf{u},\mathbf{u}}^{-1}\mathbf{K}_{\mathbf{u},\mathbf{f}} + \mathbf{D}$ in \mathcal{L}_{cVB} . Due to the structural equivalence to SCMGP, the computational complexity is calculated as $\mathcal{O}(N^3M + NMQ^2)$.

4.2. Stochastic Variational Inference

Stochastic variational inference (SVI) facilitates employing stochastic optimization algorithms in the VI framework (Hoffman et al., 2013). The crucial benefit of is enabling parallelization and hence scalability to large datasets. However, \mathcal{L}_{cVB} cannot be utilized as a stochastic variational bound, because dependencies between the observations are retained by marginalizing out \mathbf{u} .

In recent GP literature, this problem is tackled by introducing a variational distribution $q(\mathbf{u}) = \mathcal{N}(\mathbf{u}|\boldsymbol{\mu}_{\mathbf{u}}, \mathbf{S})$ (Hensman et al., 2013; Saul et al., 2016). Realizing that the first term of Eq. (9) differs from Eq. (1) via the diagonal matrix \mathbf{D} , we derive the stochastic variational bound of WSMGP in a similar manner. Specifically, the bound, denoted by

\mathcal{L}_{sVB} , is derived as

$$\mathcal{L}_{\text{sVB}} = \sum_{n=1, m=1}^{N, M} \mathbb{E}_{q(\mathbf{f}_m)} \left[\log \mathcal{N} \left([\mathbf{y}]_n \mid [\mathbf{f}_m]_n, \frac{\sigma_m^2}{[\hat{\Pi}]_{nm}} \right) \right] - \text{KL}(q(\mathbf{u}) \parallel p(\mathbf{u})) + \mathcal{V}. \quad (10)$$

The approximate marginal posterior for \mathbf{f}_m is given by $q(\mathbf{f}_m) = \int p(\mathbf{f}_m | \mathbf{u}) q(\mathbf{u}) d\mathbf{u}$ and where $q(\mathbf{f}_m) = \mathcal{N}(\mathbf{f}_m | \boldsymbol{\mu}_{q(\mathbf{f}_m)}, \boldsymbol{\Sigma}_{q(\mathbf{f}_m)})$ with

$$\begin{aligned} \boldsymbol{\mu}_{q(\mathbf{f}_m)} &= \mathbf{K}_{\mathbf{f}_m, \mathbf{u}} \mathbf{K}_{\mathbf{u}, \mathbf{u}}^{-1} \boldsymbol{\mu}, \\ \boldsymbol{\Sigma}_{q(\mathbf{f}_m)} &= \mathbf{K}_{\mathbf{f}_m, \mathbf{f}_m} + \mathbf{K}_{\mathbf{f}_m, \mathbf{u}} \mathbf{K}_{\mathbf{u}, \mathbf{u}}^{-1} (\mathbf{S} - \mathbf{K}_{\mathbf{u}, \mathbf{u}}) \mathbf{K}_{\mathbf{u}, \mathbf{u}}^{-1} \mathbf{K}_{\mathbf{u}, \mathbf{f}_m}. \end{aligned}$$

Note that \mathcal{L}_{sVB} significantly reduces the computational complexity to $\mathcal{O}(Q^3)$, i.e., complexity of inverting $\mathbf{K}_{\mathbf{u}, \mathbf{u}}$. The main advantage of this form is to enable stochastic optimization, where mini-batches are sampled and noisy gradients are calculated in the optimization of \mathcal{L}_{sVB} . Through this procedure our model can attain scalability. Detailed derivations are provided in the appendix. On the other hand, introducing $q(\mathbf{u})$ may produce a challenge in implementation: the variational distribution $q(\mathbf{u})$ is highly sensitive to hyperparameter changes. This can be handled using variational EM (Bishop, 2006), which iterates between optimizing the variational parameters and the hyperparameters.

4.3. Analysis of KL-divergence terms in \mathcal{V}

Now regarding the KL terms in Eq. (9). For the labeled data points, we can easily see that the second term in Eq. (9) encourages $\hat{\Pi}^l$ to be close to Π^l which is the prior label belief. For the unlabeled data points, the hyperparameter α_0 of Dirichlet prior plays an important role of regularization. To see this, we first note that the optimal value of variable $\hat{\alpha}$, denoted by $\hat{\alpha}^*$, is $[\hat{\alpha}^*]_{mn} = \hat{\alpha}_{nm}^* = \alpha_0 + [\hat{\Pi}]_{nm}$. Given $\hat{\alpha}^*$, the third term in Eq. (9) is expressed as $\text{KL}(q(\mathbf{Z}^u) q(\Pi^u) \parallel p(\mathbf{Z}^u | \Pi^u) p(\Pi^u | \alpha_0)) = \sum_{m, n=1}^{M, N^u} [\hat{\Pi}]_{nm} \log [\hat{\Pi}]_{nm} - \sum_{n=1}^{N^u} \left(\log \frac{B(\hat{\alpha}_{n1}^*, \dots, \hat{\alpha}_{nM}^*)}{B(\alpha_0)} \right)$.

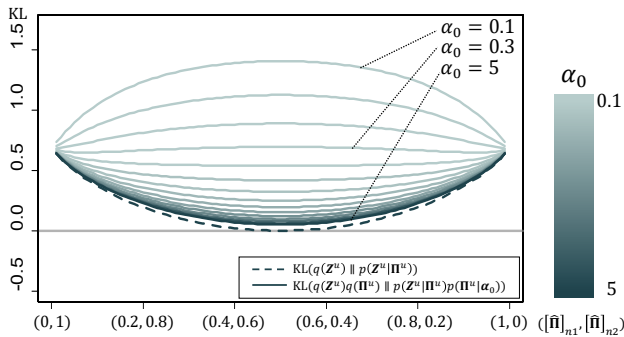


Figure 2. $\text{KL}_{\mathbf{Z}, \Pi^u}(\alpha_0)$ is convex or concave in $[\hat{\pi}]_{n1}$ depending on α_0 .

Figure 2 demonstrates the above KL-divergence corresponding to the n -th observation by $[\hat{\Pi}]_{n1}$ in the case that we consider two GPs: $\sum_{m=1,2} [\hat{\Pi}]_{nm} \log [\hat{\Pi}]_{nm} - \log \frac{B(\hat{\alpha}_{n1}^*, \hat{\alpha}_{n2}^*)}{B(\alpha_0)} = \text{KL}_{\mathbf{Z}, \Pi^u}(\alpha_0)$. Note that small $\text{KL}_{\mathbf{Z}, \Pi^u}(\alpha_0)$ is preferred in maximizing \mathcal{L}_{sVB} . According to the figure, we realize that α_0 controls the *acuteness or discretion* on assignment of observations to sources. To be more detailed, observe that if we set a large α_0 , (e.g., $\alpha_0 = 5$), then $\text{KL}_{\mathbf{Z}, \Pi^u}(\alpha_0)$ with $([\hat{\Pi}]_{n1}, [\hat{\Pi}]_{n2}) = (0, 1)$ or $(1, 0)$ is greater than the one with $([\hat{\Pi}]_{n1}, [\hat{\Pi}]_{n2}) = (0.5, 0.5)$. On the other hand, if we have a small α_0 (e.g., $\alpha_0 = 0.1$), $\text{KL}_{\mathbf{Z}, \Pi^u}(\alpha_0)$ with $([\hat{\Pi}]_{n1}, [\hat{\Pi}]_{n2}) = (0.5, 0.5)$ is greater than the one with $([\hat{\Pi}]_{n1}, [\hat{\Pi}]_{n2}) = (1, 0)$ or $(0, 1)$. Also, $\text{KL}_{\mathbf{Z}, \Pi^u}(\alpha_0)$ converges to $\text{KL}(q(\mathbf{Z}^u) \parallel p(\mathbf{Z}^u | \Pi^u))$ as α_0 increases.

Therefore, a small α_0 encourages assignment of an unlabeled observation to a group with probability close to zero or one. Thus it acts as a form of regularization or shrinkage that encourages sparse assignments, which in turn reduces predictive variance. While a large α_0 or the absence of a Dirichlet prior will augment model uncertainty via decreased acuteness in group assignments. This results also imply that the Dirichlet prior plays a role in interpretability where points can receive more acute classification results.

5. Related work

Although weakly-supervised learning has recently become a popular area within the machine learning community (e.g., Grandvalet & Bengio, 2005; Singh et al., 2009; Rohrbach et al., 2013; Ng et al., 2018), research on its interface with GPs remains sparse. The few problems that have been addressed in this area mainly focused on classification tasks using GPs (Lawrence & Jordan, 2005; Skolidis & Sanguinetti, 2013; Damianou & Lawrence., 2015). From a regression perspective, the works are numbered. Jean et al. (2018) proposed an approach based on deep kernel learning (Wilson et al., 2016) for regression with unlabeled data, inferring a posterior distribution that minimizes the variance of unlabeled data as well as labeled data. Cardona et al. (2015) modeled a convolved MGP for semi-supervised learning. Note that our model is different from such work because they define the unlabeled data as the observations of which the output value y_{nm} is missing and do not use prior knowledge or regularization for their labels.

Our study considers weakly-supervised learning for the case of missing labels for outputs rather than missing output values. In this sense, our study is closely related to Lázaro-Gredilla et al. (2012) who solve the data association problem using OMGP. The goal of data association is to infer the movement trajectories of different objects while recovering the labels identifying which trajectories correspond to which

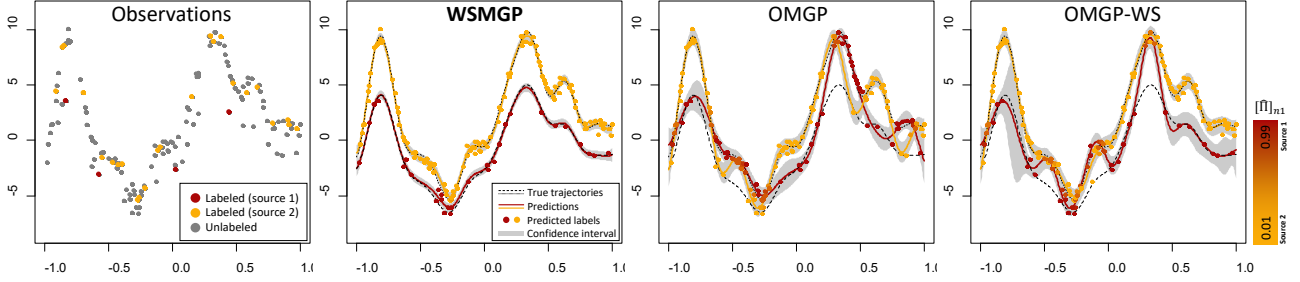


Figure 3. An illustrative example for two imbalanced populations where (imbalance ratio, labeled fraction) $=(\gamma, l) = (0.2, 0.2)$. Note that the observations from source 1 are sparse. The observed data points and labels are colored in the first panel; The same data is fitted by three models (WSMGP, OMGP, OMGP-WS) shown in the other plots where the inferred probability of each observation’s label is represented by a color gradient.

object. Extending the OMGP, Ross & Dy (2013) proposed a model that enables the inference of the number of latent GPs. Recently, Kaiser et al. (2018b) also extended the OMGP by modeling both the latent functions and the data associations using GPs. However, OMGP makes a key assumption of independence across mixture components (i.e., the outputs). This limits its capability in scenarios that calls for modeling between-output correlations and borrowing strength across outputs, a key feature we incorporate in this work. Also the previous work on the data association problem is unsupervised and cannot handle noisy labels or control labeling acuteness. Specifically, our model can search the proper hyperparameter α_0 in optimization that reduces predictive variance by acute class assignments, whereas previous models do not have any options to control, which often results in poor predictions with high variances.

6. Experimental Results

We show the experimental results to assess the performance of the proposed model using both synthetic and real-world data. We compare WSMGP to two OMGP-based benchmarks and SCMGP: (i) OMGP ((Lázaro-Gredilla et al., 2012)), where $[\mathbf{\Pi}]_{nm} = 1/M$, for any n, m (ignoring labels), (ii) weakly-supervised OMGP (OMGP-WS), where $[\mathbf{\Pi}]_{nm'} = 1$ and $[\mathbf{\Pi}]_{nm} = 0$ for $m \in \{1, \dots, M\} \setminus \{m'\}$ if $h_n = m'$, for the n -th observation (account for observed labels), (iii) SCMGP, using only labeled observations. Note that comparing WSMGP with SCMGP will show if WSMGP efficiently leverages the unlabeled data.

6.1. Experiment on Synthetic Data

For WSMGP, we use one latent process $u(\mathbf{w})$ modeled as a GP with squared exponential kernel $k_{u,u}(\mathbf{w}, \mathbf{w}') = \exp[-\frac{1}{2}(\mathbf{w} - \mathbf{w}')^T \mathbf{L}(\mathbf{w} - \mathbf{w}')$, where \mathbf{L} is a diagonal matrix. We also use the smoothing kernel $k_m(\mathbf{x} - \mathbf{w}) = \frac{S_m |\mathbf{L}_m|^{1/2}}{(2\pi)^{p/2}} \exp[-\frac{1}{2}(\mathbf{x} - \mathbf{w})^T \mathbf{L}_m(\mathbf{x} - \mathbf{w})]$ with $S_m \in \mathbb{R}$ and a positive definite matrix \mathbf{L}_m , which is widely studied

in the literature (e.g., Álvarez & Lawrence, 2011; Álvarez et al., 2019). As benchmarks, a squared exponential kernel is used for each independent GP. In the experiment using synthetic data, we assume that we have two sources ($m = 1, 2$). The data is generated from a full MGP composed of two GPs corresponding to the sources, with a kernel $k_{f_m, f_m}(\mathbf{x}, \mathbf{x}')$ where $\mathbf{L}_1 = 120, \mathbf{L}_2 = 200, S_1 = 4, S_2 = 5, \mathbf{L} = 100, \sigma_1 = \sigma_2 = 0.25$ and $Q = 30$. For each source we generate 120 observations. As in the motivating example, we consider sparse observations from source 1. We introduce γ -sparsity to indicate the ratio of the number of observations from source 1 to those from source 2. In addition, we use “ l -dense” to indicate that l fraction of the observed data from each source are labeled. The source code is provided in the appendix.

Imbalanced populations We first investigate the behavior of WSMGP when we have imbalanced populations. To do this, we set $\gamma = 0.2, 0.3, 0.5$ and $l = 0.2, 0.3, 0.5$ to mimic distinct levels of imbalance and fractions of the observed labels. For WSMGP, we set $\alpha_0 = 0.3$. We evaluate the prediction performance of each model by the root mean squared error (RMSE), where the errors are evaluated at \mathbf{x}^* . To clearly separate the two groups/sources, in the simulations, we assume a bias of $b = 2$ (a constant mean of GP) to the source 2.

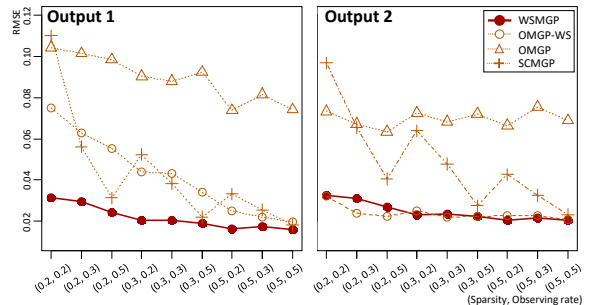


Figure 4. Mean of RMSE. Standard deviations are omitted for clear representation.

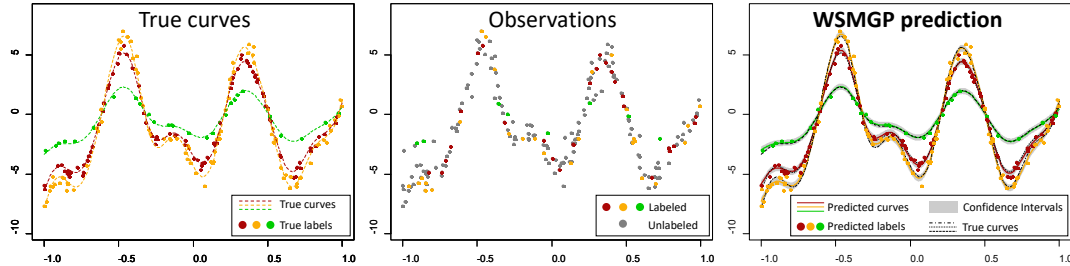


Figure 5. An illustrative example of the case where the latent functions only differ in local areas.

We make four key observations about the results shown in Figure 3 and 4. First, the WSMGP outperforms the benchmarks, especially for source 1 at low γ values (highly imbalanced populations). Therefore, WSMGP can use information of the dense group (source 2) for predicting the responses in the sparse group (source 1). In contrast, the benchmarks model the latent curves independently resulting in poor predictions for the sparse group. Importantly, WSMGP (second panel in Figure 3) infers the label of each observation with an overall higher accuracy relative to the benchmarks (third and fourth panels in Figure 3). Both better prediction and more accurate label recovery are direct benefits offered by our model’s capacity to incorporate the between group correlations. Second, Figure 4 shows that the prediction accuracy of each model improves as the population becomes more balanced with more labels (larger values of γ and l). Specifically, we did not observe significant reductions in RMSE for OMGP as the fraction of observed labels l increases. This is not surprising given OMGP ignores the labels. Third, the WSMGP outperforms SCMGP in both groups. This results illustrate the capability of WSMGP for weakly-supervised learning, which makes use of information from unlabeled data to improve predictions. Fourth, the WSMGP has small RMSEs for both sources, while the OMGP-WS cannot predict well for the sparse group 1 (Figure 4). For example, with enough number of labels or observations, the OMGP-WS can make a reasonable prediction for the dense group (see the fourth panel in Figure 3), while the predictions for the sparse group is poor. The ability of WSMGP to predict the responses well even for sparse groups highlights the potential of our model in achieving the goal of *fairness* in prediction for imbalanced groups, a direction we hope to pursue in future work.

Revealing similar latent functions In this experiment, we generate data with three outputs where two of them are very similar; we set $b = 0$. We still maintain the setting in terms of the sparsity and partially observed labels as the previous experiment. An illustrative example is represented in Figure 5. We remark that, based on the observations in the second plot, it is very difficult to distinguish the true curve of each source for a human observer. The differences

between similar curves mainly come from the peaks and valleys (e.g., $[-0.6, -0.4]$, $[-0.2, 0.2]$), and the WSMGP performs well to reveal the underlying similar curves in those intervals.

Dirichlet prior In this experiment we investigate the effect of varying the hyperparameter α_0 of the Dirichlet prior. We compare the WSMGP with $\alpha_0 = 0.3$ and an alternative model, say WSMGP-NoDir, obtained by removing the Dirichlet prior from WSMGP. A comparative result is demonstrated in Figure 6. Note that the plots in the second row represents $[\hat{\Pi}]_{n,1}$, with values close to 1 or 0 representing high levels of posterior certainty of the inferred labels.

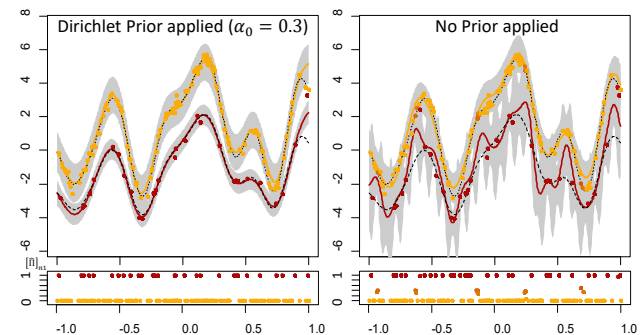


Figure 6. Predictions by WSMGP and WSMGP without Dirichlet prior. Plots in the second row illustrates the posterior probability of belonging to the source 1 for each observation ($[\hat{\Pi}]_{n,1}$).

From the second row of the figure, we can find that the WSMGP-NoDir does not assign proper probabilities to some observations which leads to a poor prediction, while WSMGP perfectly assigns the probabilities for every observation. This is because the inference of $\hat{\Pi}$ depends on the Dirichlet prior. Specifically, as we discussed in Section 4.3, if a small α_0 is given (e.g., $\alpha = 0.3$), the model is encouraged to find a probability that clearly specifies a group for unlabeled observations, and vice versa. In particular, if α_0 is large enough (e.g., $\alpha_0=100$), the WSMGP converges to WSMGP-NoDir. It shows that placing the Dirichlet prior enable WSMGP to achieve more flexibility by searching a proper α_0 , while WSMGP-NoDir does not have this option. We can treat α_0 as a hyperparameter to be optimized. Jointly

optimizing α_0 with other parameters, the model can provide a better prediction.

6.2. Experiments on Real-world Data

Housing Price Index data We apply our model and the benchmarks to the interpolation of time-series for housing prices. Specifically, we use the Housing Prices Index (HPI) datasets¹ created by Federal Housing Finance Agency (FHFA). The HPI is obtained by weighting repeat-sales index, which evaluates the variations of average price in repeat sales or refinancings on the same properties. FHFA measured the HPI based on the observations on repeat mortgage transactions of single-family properties. The dataset contains HPI of various cities in US from January 1975 to 2019, evaluated at quarterly or monthly. Note that we can expect the HPI of neighboring cities would exhibit correlation.

From the dataset we collect the HPI of two cities in state of Michigan: Ann Arbor and Kalamazoo-Portage metropolitan area. HPI for both cities are evaluated at quarterly. We randomly collected 30% of observations as a training dataset. We sparsify the observations from Ann Arbor based on $\gamma = 0.5$. Additionally, we further remove observations for Ann Arbor in a range from 2000 to 2011 for an efficient comparison of the models. Finally, We removed the labels specifying a city based on $l = 0.5$ for both cities.

Figure 7 illustrates the training data and results. According to the results, we find that the WSMGP can efficiently find the labels as well as the latent curves in the sparse range (2000 to 2011). Specifically, using the given labels, WSMGP can accurately find the latent curves in the dense area and learn the correlation between them. Based on the correlation it can find the latent curve of the sparse group (Ann Arbor). Note that OMGP-WS can find the latent curve of the dense group (Kalamazoo-Portage), whereas poorly predicts the sparse group for the sparse range in particular.

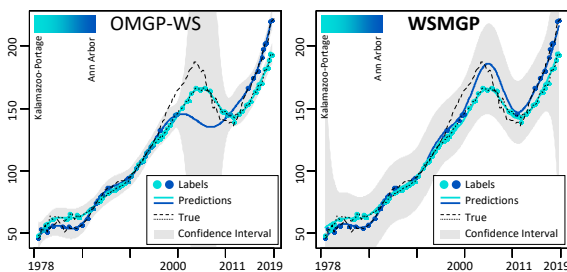


Figure 7. Predictions on HPI data.

Climate data This climate data is collected from sensor networks established in the southern coast of UK, which is composed of four sensors called as Bramblemet, Camber-

¹<https://www.fhfa.gov/DataTools/Downloads/Pages/House-Price-Index-Datasets.aspx>

met, Chimet and Sotonmet (Osborne et al., 2008; Parra & Tobar, 2017). They collect several maritime environmental signals in every 5 minutes. The signals are highly correlated across the sensors since they are set up in adjacent locations. We choose one factor, tide depth in meters, collected from Bramblemet and Chimet. we extract two consecutive days in August 2019 for each sensor. Specifically, we form 27 datasets where corresponding days are (1th, 2nd), (2nd, 3rd), ...(29th, 30th) from which two days (12th, 13th) and (13th, 14th) are excluded. We removed the two datasets since they exhibit abnormal trajectories. In particular, we sparsify the Bramblemet data with $\gamma = 0.3$ and remove 50% labels for both sensors. To obtain more challenging setting, we further remove observations of Bramblemet from 12:00am to 12:00pm in the second days. Finally, we adopt RMSE to compare performances.

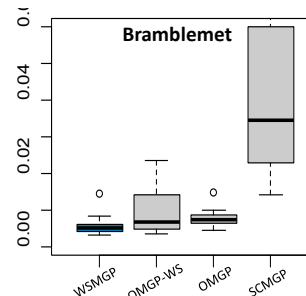


Figure 8. Boxplot for RMSE by method. Outliers are excluded.

Figure 8 summarizes the results. First of all, we find that WSMGP outperforms the benchmarks in prediction for Bramblemet with sparse observations. This shows that WSMGP reveals the missing labels well and makes a good prediction for sparse output by transferring information from the dense output. We further remark that WSMGP predicts better than SCMGP. This is because WSMGP can leverage information from unlabeled data, which demonstrates the capability of our model for weakly-supervised learning. Note that benchmarks using unlabeled data, i.e., OMGP and OMGP-WS, also outperform SCMGP.

7. Conclusion

In this study we have proposed a Bayesian probabilistic model for weakly-supervised learning that performs multi-output regression with partially labeled outputs. Through extensive simulations and empirical studies, we show the proposed approach excels in settings with imbalanced populations with correlated latent functions, which we believe are particularly relevant for improving fairness in prediction in machine learning. Even more scientific applications (e.g., Wu & Chen, 2019) need extensions of the proposed WSMGP framework for multivariate non-continuous and mixed-type outcomes which we will pursue in future work.

References

- Álvarez, M. A. and Lawrence, N. D. Computationally efficient convolved multiple output gaussian processes. *Journal of Machine Learning Research*, 12(May):1459–1500, 2011.
- Álvarez, M. A., Rosasco, L., Lawrence, N. D., et al. Kernels for vector-valued functions: A review. *Foundations and Trends® in Machine Learning*, 4(3):195–266, 2012.
- Álvarez, M. A., Luengo, D., and Lawrence, N. D. Linear latent force models using gaussian processes. *IEEE transactions on pattern analysis and machine intelligence*, 35(11):2693–2705, 2013.
- Álvarez, M. A., Ward, W. O. C., and Guarnizo, C. Non-linear process convolutions for multi-output gaussian processes. In *International Conference on Artificial Intelligence and Statistics*, pp. 1969–1977, 2019.
- Bishop, C. M. *Pattern recognition and machine learning*. springer, 2006.
- Blei, D. M., Kucukelbir, A., and McAuliffe, J. D. Variational inference: A review for statisticians. *Journal of the American Statistical Association*, 112(518):859–877, 2017.
- Burt, D. R., Rasmussen, C. E., and Van Der Wilk, M. Rates of convergence for sparse variational gaussian process regression. In *Proceedings of the 36th International Conference on Machine Learning*, pp. 862–871, 2019.
- Cardona, H. D. V., Álvarez, M. A., and Orozco, Á. A. Convolved multi-output gaussian processes for semi-supervised learning. In *International Conference on Image Analysis and Processing*, pp. 109–118. Springer, 2015.
- Dai, Z., Álvarez, M. A., and Lawrence, N. Efficient modeling of latent information in supervised learning using gaussian processes. In *Advances in Neural Information Processing Systems*, pp. 5131–5139, 2017.
- Damianou, A. and Lawrence, N. D. Semi-described and semi-supervised learning with gaussian processes. In *Uncertainty in Artificial Intelligence (UAI)*, 2015.
- Fricker, T. E., Oakley, J. E., and Urban, N. M. Multivariate gaussian process emulators with nonseparable covariance structures. *Technometrics*, 55(1):47–56, 2013.
- Grandvalet, Y. and Bengio, Y. Semi-supervised learning by entropy minimization. In *Advances in neural information processing systems*, pp. 529–536, 2005.
- Hensman, J., Fusi, N., and Lawrence, N. D. Gaussian processes for big data. *Conference on Uncertainty in Artificial Intelligence*, pp. 282–290, 2013.
- Hoffman, M. D., Blei, D. M., Wang, C., and Paisley, J. Stochastic variational inference. *The Journal of Machine Learning Research*, 14(1):1303–1347, 2013.
- Jean, N., Xie, S. M., and Ermon, S. Semi-supervised deep kernel learning: Regression with unlabeled data by minimizing predictive variance. In *Neural Information Processing Systems*, 2018.
- Kaiser, M., Otte, C., Runkler, T., and Ek, C. H. Bayesian alignments of warped multi-output gaussian processes. In *Advances in Neural Information Processing Systems*, pp. 6995–7004, 2018a.
- Kaiser, M., Otte, C., Runkler, T. A., and Ek, C. H. Data association with gaussian processes. In *ArXiv preprint*, 2018b.
- King, N. J. and Lawrence, N. D. Fast variational inference for gaussian process models through kl-correction. In *European Conference on Machine Learning*, pp. 270–281. Springer, 2006.
- Kontar, R., Zhou, S., Sankavaram, C., Du, X., and Zhang, Y. Nonparametric modeling and prognosis of condition monitoring signals using multivariate gaussian convolution processes. *Technometrics*, 60(4):484–496, 2018.
- Lawrence, N. D. and Jordan, M. I. Semi-supervised learning via gaussian processes. In *Advances in neural information processing systems*, pp. 753–760, 2005.
- Lázaro-Gredilla, M., Van Vaerenbergh, S., and Lawrence, N. D. Overlapping mixtures of gaussian processes for the data association problem. *Pattern Recognition*, 45(4):1386–1395, 2012.
- Ng, Y. C., Colombo, N., and Silva, R. Bayesian semi-supervised learning with graph gaussian processes. In *Advances in Neural Information Processing Systems*, pp. 1683–1694, 2018.
- Osborne, M. A., Roberts, S. J., Rogers, A., Ramchurn, S. D., and Jennings, N. R. Towards real-time information processing of sensor network data using computationally efficient multi-output gaussian processes. In *2008 International Conference on Information Processing in Sensor Networks (ipsn 2008)*, pp. 109–120. IEEE, 2008.
- Panos, A., Dellaportas, P., and Titsias, M. K. Fully scalable gaussian processes using subspace inducing inputs. *arXiv preprint arXiv:1807.02537*, 2018.
- Parra, G. and Tobar, F. Spectral mixture kernels for multi-output gaussian processes. In *Advances in Neural Information Processing Systems*, pp. 6681–6690, 2017.

- Quiñonero-Candela, J. and Rasmussen, C. E. A unifying view of sparse approximate gaussian process regression. *Journal of Machine Learning Research*, 6(Dec):1939–1959, 2005.
- Rohrbach, M., Ebert, S., and Schiele, B. Transfer learning in a transductive setting. In *Advances in neural information processing systems*, pp. 46–54, 2013.
- Ross, J. and Dy, J. Nonparametric mixture of gaussian processes with constraints. In *International Conference on Machine Learning*, pp. 1346–1354, 2013.
- Saul, A. D., Hensman, J., Vehtari, A., and Lawrence, N. D. Chained gaussian processes. In *Artificial Intelligence and Statistics*, pp. 1431–1440, 2016.
- Singh, A., Nowak, R., and Zhu, J. Unlabeled data: Now it helps, now it doesn't. In *Advances in neural information processing systems*, pp. 1513–1520, 2009.
- Skolidis, G. and Sanguinetti, G. Semisupervised multitask learning with gaussian processes. *IEEE transactions on neural networks and learning systems*, 24(12):2101–2112, 2013.
- Titsias, M. Variational learning of inducing variables in sparse gaussian processes. In *Artificial Intelligence and Statistics*, pp. 567–574, 2009.
- Wilson, A. G., Hu, Z., Salakhutdinov, R., and Xing, E. P. Deep kernel learning. In *Artificial Intelligence and Statistics*, pp. 370–378, 2016.
- Wu, Z. and Chen, I. Regression analysis of dependent binary data for estimating disease etiology from case-control studies. *arXiv preprint arXiv:1906.08436*, 2019.
- Zhao, J. and Sun, S. Variational dependent multi-output gaussian process dynamical systems. *The Journal of Machine Learning Research*, 17(1):4134–4169, 2016.
- Zhou, Z.-H. A brief introduction to weakly supervised learning. *National Science Review*, 5(1):44–53, 2017.

A. Derivations of variational bounds

A.1. Derivations of \mathcal{L}_{cVB}

Here we use the same notations as in the main article. For notational simplicity, we omit hyperparameters $\{\boldsymbol{\theta}, \boldsymbol{\alpha}_0\}$ in the derivations unless it causes confusion. We use the notation $\mathbb{E}_{\mathbf{a}}[\cdot]$ to indicate expectation over a variational distribution $q(\mathbf{a})$.

First, we start with calculating the following expectation that will be used shortly:

$$\begin{aligned}
 \mathbb{E}_{\mathbf{Z}}[\log p(\mathbf{y}|\mathbf{f}, \mathbf{Z})] &= \mathbb{E}_{\mathbf{Z}} \left[\sum_{n=1, m=1}^{N, M} [\mathbf{Z}]_{nm} \log \mathcal{N}(\mathbf{y}_n | [\mathbf{f}_m]_n, \sigma_m^2) \right] \\
 &= \sum_{n=1, m=1}^{N, M} [\hat{\boldsymbol{\Pi}}]_{nm} \log \mathcal{N}(\mathbf{y}_n | [\mathbf{f}_m]_n, \sigma_m^2) \\
 &= \sum_{n=1, m=1}^{N, M} \log \mathcal{N}(\mathbf{y}_n | [\mathbf{f}_m]_n, \frac{\sigma_m^2}{[\hat{\boldsymbol{\Pi}}]_{nm}}) + \frac{1}{2} \sum_{n=1, m=1}^{N, M} \log \frac{(2\pi\sigma_m^2)^{(1-[\hat{\boldsymbol{\Pi}}]_{nm})}}{[\hat{\boldsymbol{\Pi}}]_{nm}}. \\
 &= \log \mathcal{N}(\mathbf{y}|\mathbf{f}, \mathbf{D}) + \frac{1}{2} \sum_{n=1, m=1}^{N, M} \log \frac{(2\pi\sigma_m^2)^{(1-[\hat{\boldsymbol{\Pi}}]_{nm})}}{[\hat{\boldsymbol{\Pi}}]_{nm}}.
 \end{aligned} \tag{A1}$$

Now we derive \mathcal{L}_{cVB} . Recall that we have

$$\mathcal{L}_{\text{cVB}} = \log \int_{\mathbf{f}, \mathbf{u}} \left(e^{\int_{\mathbf{Z}, \boldsymbol{\Pi}^u} q(\mathbf{Z})q(\boldsymbol{\Pi}^u) \log \frac{p(\mathbf{y}|\mathbf{f}, \mathbf{Z})p(\mathbf{Z}|\boldsymbol{\Pi})p(\boldsymbol{\Pi}^u)}{q(\mathbf{Z})q(\boldsymbol{\Pi}^u)} p(\mathbf{f}|\mathbf{u}, \mathbf{X}, \mathbf{W})p(\mathbf{u}|\mathbf{W})} \right) \leq \log p(\mathbf{y}|\mathbf{X}, \mathbf{W}). \tag{A2}$$

In Eq. (A2), we first focus on the following integral on the exponential

$$\begin{aligned}
 &\int_{\mathbf{Z}, \boldsymbol{\Pi}^u} q(\mathbf{Z})q(\boldsymbol{\Pi}^u) \log \frac{p(\mathbf{y}|\mathbf{f}, \mathbf{Z})p(\mathbf{Z}|\boldsymbol{\Pi})p(\boldsymbol{\Pi}^u)}{q(\mathbf{Z})q(\boldsymbol{\Pi}^u)} \\
 &= \mathbb{E}_{\mathbf{Z}}[\log p(\mathbf{y}|\mathbf{f}, \mathbf{Z})] - \text{KL}(q(\mathbf{Z}^l) \| p(\mathbf{Z}^l | \boldsymbol{\Pi}^l)) - \text{KL}(q(\mathbf{Z}^u)q(\boldsymbol{\Pi}^u) \| p(\mathbf{Z}^u | \boldsymbol{\Pi}^u)p(\boldsymbol{\Pi}^u)) \\
 &= \log \mathcal{N}(\mathbf{y}|\mathbf{f}, \mathbf{D}) + \mathcal{V}
 \end{aligned} \tag{A3}$$

where the last identity is based on Eq. (A1) and the terms for $\mathbf{Z}, \boldsymbol{\Pi}$ are collected into

$$\mathcal{V} = -\text{KL}(q(\mathbf{Z}^l) \| p(\mathbf{Z}^l | \boldsymbol{\Pi}^l)) - \text{KL}(q(\mathbf{Z}^u)q(\boldsymbol{\Pi}^u) \| p(\mathbf{Z}^u | \boldsymbol{\Pi}^u)p(\boldsymbol{\Pi}^u)) + \frac{1}{2} \sum_{n=1, m=1}^{N, M} \log \frac{(2\pi\sigma_m^2)^{(1-[\hat{\boldsymbol{\Pi}}]_{nm})}}{[\hat{\boldsymbol{\Pi}}]_{nm}}.$$

Plugging Eq. (A3) into Eq. (A2), we obtain the final form of \mathcal{L}_{cVB} as

$$\begin{aligned}
 \mathcal{L}_{\text{cVB}} &= \log \int_{\mathbf{f}, \mathbf{u}} \left(e^{\int_{\mathbf{Z}, \boldsymbol{\Pi}^u} q(\mathbf{Z})q(\boldsymbol{\Pi}^u) \log \frac{p(\mathbf{y}|\mathbf{f}, \mathbf{Z})p(\mathbf{Z}|\boldsymbol{\Pi})p(\boldsymbol{\Pi}^u)}{q(\mathbf{Z})q(\boldsymbol{\Pi}^u)} p(\mathbf{f}|\mathbf{u}, \mathbf{X}, \mathbf{W})p(\mathbf{u}|\mathbf{W})} \right) \\
 &= \log \int_{\mathbf{f}, \mathbf{u}} \mathcal{N}(\mathbf{y}|\mathbf{f}, \mathbf{D})p(\mathbf{f}|\mathbf{u}, \mathbf{X}, \mathbf{W})p(\mathbf{u}|\mathbf{W}) + \mathcal{V} \\
 &= \log \mathcal{N}(\mathbf{y}|\mathbf{0}, \mathbf{B} + \mathbf{K}_{\mathbf{f}, \mathbf{u}}\mathbf{K}_{\mathbf{u}, \mathbf{u}}^{-1}\mathbf{K}_{\mathbf{u}, \mathbf{f}} + \mathbf{D}) + \mathcal{V}
 \end{aligned} \tag{A4}$$

of which the last inequality is based on Eq. (1) in the main article.

A.2. Derivations of \mathcal{L}_{sVB}

To obtain the scalable variational bound \mathcal{L}_{sVB} , we further introduce $q(\mathbf{u}) = \mathcal{N}(\boldsymbol{\mu}_{\mathbf{u}}, \mathbf{S})$ to approximate $p(\mathbf{u})$. We first derive the variational marginalized distribution for \mathbf{f}_m as

$$q(\mathbf{f}_m) = \int_{\mathbf{u}} q(\mathbf{f}_m, \mathbf{u}) = \int_{\mathbf{u}} p(\mathbf{f}_m|\mathbf{u}, \mathbf{X}, \mathbf{W})q(\mathbf{u}) = \mathcal{N}(\mathbf{K}_{\mathbf{f}_m, \mathbf{u}}\mathbf{K}_{\mathbf{u}, \mathbf{u}}\boldsymbol{\mu}_{\mathbf{u}}, \mathbf{K}_{\mathbf{f}_m, \mathbf{f}_m} + \mathbf{K}_{\mathbf{f}_m, \mathbf{u}}\mathbf{K}_{\mathbf{u}, \mathbf{u}}^{-1}(\mathbf{S} - \mathbf{K}_{\mathbf{u}, \mathbf{u}})\mathbf{K}_{\mathbf{u}, \mathbf{u}}^{-1}\mathbf{K}_{\mathbf{u}, \mathbf{f}_m}).$$

Then, the lower bound \mathcal{L}_{sVB} is given by

$$\begin{aligned}\mathcal{L}_{\text{sVB}} &= \int_{\mathbf{f}, \mathbf{u}, \mathbf{Z}, \mathbf{\Pi}} q(\mathbf{f}, \mathbf{u})q(\mathbf{Z})q(\mathbf{\Pi}^u) \log \frac{p(\mathbf{y}|\mathbf{f}, \mathbf{Z})p(\mathbf{f}|\mathbf{u}, \mathbf{X}, \mathbf{W})p(\mathbf{u}|\mathbf{W})p(\mathbf{Z}|\mathbf{\Pi})p(\mathbf{\Pi}^u)}{q(\mathbf{f}, \mathbf{u})q(\mathbf{Z})q(\mathbf{\Pi}^u)} \\ &= \mathbb{E}_{\mathbf{f}} [\mathbb{E}_{\mathbf{Z}} [\log p(\mathbf{y}|\mathbf{f}, \mathbf{Z})]] - \text{KL}(q(\mathbf{u})\|p(\mathbf{u})) - \text{KL}(q(\mathbf{Z}^l)\|p(\mathbf{Z}^l|\mathbf{\Pi}^l)) - \text{KL}(q(\mathbf{Z}^u)q(\mathbf{\Pi}^u)\|p(\mathbf{Z}^u|\mathbf{\Pi}^u)p(\mathbf{\Pi}^u)) \\ &= \mathbb{E}_{\mathbf{f}} [\log \mathcal{N}(\mathbf{y}|\mathbf{f}, \mathbf{D})] - \text{KL}(q(\mathbf{u})\|p(\mathbf{u})) + \mathcal{V},\end{aligned}$$

where we use the variational expectation Eq. (A1) for the last identity. We recover Eq. (10) by noting that $\log \mathcal{N}(\mathbf{y}|\mathbf{f}, \mathbf{D}) = \sum_{n=1, m=1}^{N, M} \log \mathcal{N}([\mathbf{y}]_n | [\mathbf{f}]_m, \frac{\sigma_m^2}{[\hat{\mathbf{\Pi}}]_{nm}})$ because \mathbf{D} is a diagonal matrix.

B. Gradients of Variational Bounds

To utilize gradient-based optimization algorithms, we provide the gradients of proposed variational bounds for the parameters. In \mathcal{L}_{cVB} , the parameters to be optimized are: $\boldsymbol{\theta}$, $\boldsymbol{\sigma}$, α_0 , $\hat{\mathbf{\Pi}}$ and \mathbf{W} , where $\boldsymbol{\theta}$ collects the hyperparameters related to the GPs $p(\mathbf{f}|\mathbf{X})$ and $p(\mathbf{u}|\mathbf{W})$, denoted by $\boldsymbol{\theta}_{\mathbf{f}}$ and $\boldsymbol{\theta}_{\mathbf{u}}$, respectively. In \mathcal{L}_{sVB} , we additionally have $\boldsymbol{\mu}_{\mathbf{u}}$ and \mathbf{S} .

We first consider \mathcal{V} that appears in both \mathcal{L}_{cVB} and \mathcal{L}_{sVB} . The related parameters are α_0 and $\hat{\mathbf{\Pi}}$, that is, α_0 and $[\hat{\mathbf{\Pi}}]_{nm}$ for $n = 1, \dots, N$ and $m = 1, \dots, M$. Because \mathcal{V} can be expressed as the summation in which terms are independent of each other in terms of the parameters, it is trivial to derive the partial derivatives; we omit the derivatives of \mathcal{V} .

The remaining terms are a bit tricky to obtain partial derivatives since they include matrices. In order to obtain the partial derivatives for the parameters in matrix, we use the notation of $\mathbf{?}$: we define $\mathbf{G}_{\mathbf{?}}$, which denotes a vector obtained by vectorizing the matrix \mathbf{G} . The partial derivative for each parameter is calculated using the law of total derivative and the chain rule. For example, consider $\boldsymbol{\theta}_{\mathbf{f}}$ in \mathcal{L}_{cVB} . The matrices that involve $\boldsymbol{\theta}_{\mathbf{f}}$ are $\mathbf{K}_{\mathbf{f}, \mathbf{u}}$ and $\mathbf{K}_{\mathbf{f}, \mathbf{f}}$. Hence, the partial derivative of $\boldsymbol{\theta}_{\mathbf{f}}$ is given by $\frac{\partial \mathcal{L}_{\text{cVB}}}{\partial \boldsymbol{\theta}_{\mathbf{f}}} = \frac{\partial \mathcal{L}_{\text{cVB}}}{\partial \mathbf{K}_{\mathbf{f}, \mathbf{u}}} \frac{\partial \mathbf{K}_{\mathbf{f}, \mathbf{u}}}{\partial \boldsymbol{\theta}_{\mathbf{f}}} + \frac{\partial \mathcal{L}_{\text{cVB}}}{\partial \mathbf{K}_{\mathbf{f}, \mathbf{f}}} \frac{\partial \mathbf{K}_{\mathbf{f}, \mathbf{f}}}{\partial \boldsymbol{\theta}_{\mathbf{f}}}$. In the following sections, we find the partial derivatives of the proposed lowerbounds for each matrix.

B.1. Matrix Derivatives of \mathcal{L}_{cVB}

Let $\mathcal{L}_{\text{cVB}}^{(1)}$ denote the first term in \mathcal{L}_{cVB} , $\log \mathcal{N}(\mathbf{y}|\mathbf{0}, \mathbf{B} + \mathbf{K}_{\mathbf{f}, \mathbf{u}}\mathbf{K}_{\mathbf{u}, \mathbf{u}}^{-1}\mathbf{K}_{\mathbf{u}, \mathbf{f}} + \mathbf{D})$. Note that this is structurally equivalent to the marginal distribution of sparse convolved multi-output GP (1) proposed by [Álvarez & Lawrence \(2011\)](#). Our derivation is similar to their work, we thus directly provide the results. A reader who wants to find detailed derivations is referred to the supplement of [Álvarez & Lawrence \(2011\)](#).

$$\begin{aligned}\frac{\partial \mathcal{L}_{\text{cVB}}^{(1)}}{\partial \mathbf{K}_{\mathbf{f}, \mathbf{f}}} &= \frac{\partial \mathcal{L}_{\text{cVB}}^{(1)}}{\partial \mathbf{D}} = -\frac{1}{2} (\mathbf{Q}_{\mathbf{?}})^{\top}, \\ \frac{\partial \mathcal{L}_{\text{cVB}}^{(1)}}{\partial \mathbf{K}_{\mathbf{u}, \mathbf{f}}} &= ((\mathbf{K}_{\mathbf{u}, \mathbf{u}}^{-1}\mathbf{K}_{\mathbf{u}, \mathbf{f}}\mathbf{Q} - \mathbf{C}\mathbf{K}_{\mathbf{u}, \mathbf{f}}\mathbf{B}^{-1} + \mathbf{A}^{-1}\mathbf{K}_{\mathbf{u}, \mathbf{f}}\mathbf{B}^{-1}\mathbf{y}\mathbf{y}^{\top}\mathbf{B}^{-1})_{\mathbf{?}})^{\top}, \\ \frac{\partial \mathcal{L}_{\text{cVB}}^{(1)}}{\partial \mathbf{K}_{\mathbf{u}, \mathbf{u}}} &= -\frac{1}{2} ((\mathbf{K}_{\mathbf{u}, \mathbf{u}}^{-1} - \mathbf{C} - \mathbf{K}_{\mathbf{u}, \mathbf{u}}^{-1}\mathbf{K}_{\mathbf{u}, \mathbf{f}}\mathbf{Q}\mathbf{K}_{\mathbf{f}, \mathbf{u}}\mathbf{K}_{\mathbf{u}, \mathbf{u}}^{-1})_{\mathbf{?}})^{\top},\end{aligned}$$

with $\mathbf{A} = \mathbf{K}_{\mathbf{u}, \mathbf{u}} + \mathbf{K}_{\mathbf{u}, \mathbf{f}}(\mathbf{B} + \mathbf{D})^{-1}\mathbf{K}_{\mathbf{f}, \mathbf{u}}$; $\mathbf{Q} = (\mathbf{B}^{-1}\mathbf{J}\mathbf{B}^{-1} \odot \mathbf{P})$; $\mathbf{J} = \mathbf{B} - \mathbf{y}\mathbf{y}^{\top} + \mathbf{K}_{\mathbf{f}, \mathbf{u}}\mathbf{A}^{-1}\mathbf{K}_{\mathbf{u}, \mathbf{f}}\mathbf{B}^{-1}\mathbf{y}\mathbf{y}^{\top} + (\mathbf{K}_{\mathbf{f}, \mathbf{u}}\mathbf{A}^{-1}\mathbf{K}_{\mathbf{u}, \mathbf{f}}\mathbf{B}^{-1}\mathbf{y}\mathbf{y}^{\top})^{\top} - \mathbf{K}_{\mathbf{f}, \mathbf{u}}\mathbf{C}\mathbf{K}_{\mathbf{u}, \mathbf{f}}$; $\mathbf{C} = \mathbf{A}^{-1} + \mathbf{A}^{-1}\mathbf{K}_{\mathbf{u}, \mathbf{f}}\mathbf{B}^{-1}\mathbf{y}\mathbf{y}^{\top}\mathbf{B}^{-1}\mathbf{K}_{\mathbf{f}, \mathbf{u}}\mathbf{A}^{-1}$, where \odot is the Hadamard product and $\mathbf{P} = \mathbf{I}_M \otimes \mathbf{1}_{N \times N}$, where $\mathbf{1}_{N \times N}$ denotes the $N \times N$ matrix with ones and \otimes is the Kronecker product.

B.2. Matrix Derivatives of \mathcal{L}_{sVB}

For notational simplicity, let us define $\mathcal{L}_{\text{sVB}}^{(1)} = \mathbb{E}_{\mathbf{f}} [\log \mathcal{N}(\mathbf{y}|\mathbf{f}, \mathbf{D})]$ and $\mathcal{L}_{\text{sVB}}^{(2)} = \text{KL}(q(\mathbf{u})\|p(\mathbf{u}))$, which are the first and second term in, respectively. That is, $\mathcal{L}_{\text{sVB}} = \mathcal{L}_{\text{sVB}}^{(1)} - \mathcal{L}_{\text{sVB}}^{(2)} + \mathcal{V}$. We need to find (i) the matrix partial derivatives for $\mathcal{L}_{\text{sVB}}^{(1)}$: $\frac{\partial \mathcal{L}_{\text{sVB}}^{(1)}}{\partial \boldsymbol{\mu}_{\mathbf{u}}}$, $\frac{\partial \mathcal{L}_{\text{sVB}}^{(1)}}{\partial \mathbf{S}}$, $\frac{\partial \mathcal{L}_{\text{sVB}}^{(1)}}{\partial \mathbf{K}_{\mathbf{u}, \mathbf{u}}}$, and (ii) the matrix partial derivatives for $\mathcal{L}_{\text{sVB}}^{(2)}$: $\frac{\partial \mathcal{L}_{\text{sVB}}^{(2)}}{\partial \boldsymbol{\mu}_{\mathbf{u}}}$, $\frac{\partial \mathcal{L}_{\text{sVB}}^{(2)}}{\partial \mathbf{S}}$, $\frac{\partial \mathcal{L}_{\text{sVB}}^{(2)}}{\partial \mathbf{K}_{\mathbf{u}, \mathbf{u}}}$, $\frac{\partial \mathcal{L}_{\text{sVB}}^{(2)}}{\partial \mathbf{K}_{\mathbf{u}, \mathbf{f}}}$, $\frac{\partial \mathcal{L}_{\text{sVB}}^{(2)}}{\partial \text{diag}(\mathbf{K}_{\mathbf{f}, \mathbf{f}})}$, $\frac{\partial \mathcal{L}_{\text{sVB}}^{(2)}}{\partial \text{diag}(\mathbf{D})}$. To

do this, we are first required to find the derivatives of the variational expectation

$$\begin{aligned}\frac{\partial}{\partial \boldsymbol{\mu}_{q(f_m)}} \mathbb{E}_{\mathbf{f}_m} [\log \mathcal{N}(\mathbf{y}_m | \mathbf{f}_m, \mathbf{D}_m)] &= (\mathbf{y}_m - \boldsymbol{\mu}_{q(f_m)}) \odot \text{diag}(\mathbf{D}_m), \\ \frac{\partial}{\partial \boldsymbol{\Sigma}_{q(f_m)}} \mathbb{E}_{\mathbf{f}_m} [\log \mathcal{N}(\mathbf{y}_m | \mathbf{f}_m, \mathbf{D}_m)] &= -\frac{1}{2} \text{diag}(\tilde{\mathbf{D}}_m)\end{aligned}$$

where $\tilde{\mathbf{D}}_m$ represents the Hadamard reciprocal of \mathbf{D}_m . Setting $\frac{\partial}{\partial \boldsymbol{\mu}_{q(f_m)}} \mathbb{E}_{\mathbf{f}_m} [\log \mathcal{N}(\mathbf{y}_m | \mathbf{f}_m, \mathbf{D}_m)] = \mathbf{a}_m$ and $\frac{\partial}{\partial \boldsymbol{\Sigma}_{q(f_m)}} \mathbb{E}_{\mathbf{f}_m} [\log \mathcal{N}(\mathbf{y}_m | \mathbf{f}_m, \mathbf{D}_m)] = \mathbf{v}_m$, then the partial matrix derivatives for $\mathcal{L}_{\text{sVB}}^{(1)}$ and $\mathcal{L}_{\text{sVB}}^{(2)}$ are derived as

$$\begin{aligned}\frac{\partial \mathcal{L}_{\text{sVB}}^{(1)}}{\partial \boldsymbol{\mu}_{\mathbf{u}}} &= \sum_{m=1}^M (\mathbf{K}_{\mathbf{u},\mathbf{u}}^{-1} \mathbf{K}_{\mathbf{u},\mathbf{f}_m} \mathbf{a}_m) \\ \frac{\partial \mathcal{L}_{\text{sVB}}^{(1)}}{\partial \mathbf{S}} &= \left(\left(\sum_{m=1}^M \mathbf{H}_m \right) : \right)^\top \\ \frac{\partial \mathcal{L}_{\text{sVB}}^{(1)}}{\partial \mathbf{K}_{\mathbf{u},\mathbf{u}}} &= \frac{1}{2} ((\mathbf{R} + \mathbf{R}^\top) :)^\top \\ \frac{\partial \mathcal{L}_{\text{sVB}}^{(1)}}{\partial \mathbf{K}_{\mathbf{u},\mathbf{f}_m}} &= \left(\left(\mathbf{K}_{\mathbf{u},\mathbf{u}}^{-1} \boldsymbol{\mu}_{\mathbf{u}} \mathbf{a}_m^\top + 2 (\mathbf{S} \mathbf{K}_{\mathbf{u},\mathbf{u}}^{-1} - \mathbf{I}_{Q \times Q})^\top \mathbf{O}_m \right) : \right)^\top \\ \frac{\partial \mathcal{L}_{\text{sVB}}^{(1)}}{\partial \text{diag}(\mathbf{K}_{\mathbf{f}_m, \mathbf{f}_m})} &= \mathbf{v}_m \\ \frac{\partial \mathcal{L}_{\text{sVB}}^{(1)}}{\partial \text{diag}(\mathbf{D}_m)} &= \frac{1}{2} (\mathbf{v}_m + (\mathbf{y}_m \odot \mathbf{y}_m + \boldsymbol{\mu}_{\mathbf{u}} \odot \boldsymbol{\mu}_{\mathbf{u}} + \text{diag}(\boldsymbol{\Sigma}_{q(f_m)}) - 2\boldsymbol{\mu}_{\mathbf{u}} \odot \mathbf{y}_m) \odot \text{diag}(\mathbf{D}_m \odot \mathbf{D}_m))\end{aligned}$$

and

$$\begin{aligned}\frac{\partial \mathcal{L}_{\text{sVB}}^{(2)}}{\partial \boldsymbol{\mu}_{\mathbf{u}}} &= \mathbf{K}_{\mathbf{u},\mathbf{u}}^{-1} \boldsymbol{\mu}_{\mathbf{u}}, \\ \frac{\partial \mathcal{L}_{\text{sVB}}^{(2)}}{\partial \mathbf{S}} &= \frac{1}{2} ((\mathbf{K}_{\mathbf{u},\mathbf{u}}^{-1} - \mathbf{S}) :)^\top \\ \frac{\partial \mathcal{L}_{\text{sVB}}^{(2)}}{\partial \mathbf{K}_{\mathbf{u},\mathbf{u}}} &= \frac{1}{2} ((-\mathbf{K}_{\mathbf{u},\mathbf{u}}^{-1} \mathbf{S} \mathbf{K}_{\mathbf{u},\mathbf{u}}^{-1})^\top - (\mathbf{K}_{\mathbf{u},\mathbf{u}}^{-1})^\top \boldsymbol{\mu}_{\mathbf{u}} \boldsymbol{\mu}_{\mathbf{u}}^\top (\mathbf{K}_{\mathbf{u},\mathbf{u}}^{-1})^\top + (\mathbf{K}_{\mathbf{u},\mathbf{u}}^{-1})^\top)^\top,\end{aligned}$$

where $\mathbf{H}_m = \mathbf{O}_m \mathbf{K}_{\mathbf{f}_m, \mathbf{u}} \mathbf{K}_{\mathbf{u}, \mathbf{u}}^{-1}$; $\mathbf{O}_m = \mathbf{K}_{\mathbf{u}, \mathbf{u}}^{-1} \mathbf{K}_{\mathbf{u}, \mathbf{f}_m} \odot (\mathbf{1}_{Q \times 1} \otimes \mathbf{v}_m^\top)$; $\mathbf{R} = \sum_{m=1}^M (\mathbf{H}_m - \mathbf{H}_m \mathbf{S} \mathbf{K}_{\mathbf{u}, \mathbf{u}}^{-1} - (\mathbf{H}_m \mathbf{S} \mathbf{K}_{\mathbf{u}, \mathbf{u}}^{-1})^\top - \mathbf{K}_{\mathbf{u}, \mathbf{u}}^{-1} \mathbf{K}_{\mathbf{u}, \mathbf{f}_m} \mathbf{a}_m (\mathbf{K}_{\mathbf{u}, \mathbf{u}}^{-1} \boldsymbol{\mu}_{\mathbf{u}})^\top)$

C. Prediction

We may be interested in the posterior distribution of each output in WSMGP at a new input \mathbf{x}^* . Similar to the (cross-)covariance matrices we defined in SCMGP, we define the matrices evaluated at \mathbf{x}^* : $\mathbf{K}_{\mathbf{f}^*, \mathbf{f}^*}$ and $\mathbf{K}_{\mathbf{f}^*, \mathbf{u}} = \mathbf{K}_{\mathbf{u}, \mathbf{f}^*}^\top$. The posterior distribution of the m -th output is expressed as $p(\mathbf{y}^* | \mathbf{x}^*, \mathbf{y}, \mathbf{X}, \mathbf{W}, \boldsymbol{\theta}, [\hat{\boldsymbol{\Pi}}]_m, [\hat{\boldsymbol{\alpha}}]_m) = \mathcal{N}(\boldsymbol{\mu}_m^*, \boldsymbol{\Sigma}_m^*)$, where

$$\begin{aligned}\boldsymbol{\mu}_m^* &= \mathbf{K}_{\mathbf{f}_m^*, \mathbf{u}} \mathbf{A}^{-1} \mathbf{K}_{\mathbf{u}, \mathbf{f}_m} (\mathbf{B}_m + \mathbf{D}_m)^{-1} \mathbf{y} \\ \boldsymbol{\Sigma}_m^* &= \mathbf{B}_m^* + \mathbf{K}_{\mathbf{f}_m^*, \mathbf{u}} \mathbf{A}^{-1} \mathbf{K}_{\mathbf{u}, \mathbf{f}_m^*} + \sigma_m^2 \mathbf{I}_N,\end{aligned}$$

with $\mathbf{B}_m^* = \mathbf{K}_{\mathbf{f}_m^*, \mathbf{f}_m^*} - \mathbf{K}_{\mathbf{f}_m^*, \mathbf{u}} \mathbf{K}_{\mathbf{u}, \mathbf{u}}^{-1} \mathbf{K}_{\mathbf{u}, \mathbf{f}_m^*}$.

D. Additional Discussion on the Variational Bound \mathcal{L}_{cVB}

Ease applying an alternative MGP Note that in the lower bound \mathcal{L}_{cVB} , any alternative approximation of \mathbf{K} can be easily utilized in our model. For in an exact GP setting modeled in Eq. (3), the $\mathcal{L}_{\text{cVB}}(\mathbf{K})$ in Eq. (9) will have an updated first term equal to $\mathcal{N}(\mathbf{y} | \mathbf{0}, \mathbf{K} + \mathbf{D})$.

Interpretability We here recall that the diagonals of \mathbf{D} are comprised of $\mathbf{D}_1, \dots, \mathbf{D}_M$, corresponding to the GPs $\mathbf{f}_1, \dots, \mathbf{f}_M$. Now, suppose that the n -th observation is highly likely to be assigned to \mathbf{f}_m , so $[\hat{\mathbf{\Pi}}]_{nm} \rightarrow 1$. Then, we have $\sigma_m^2/[\hat{\mathbf{\Pi}}]_{nm} \rightarrow \sigma_m^2$. This also implies that $[\hat{\mathbf{\Pi}}]_{Nm'} \rightarrow 0$ for $m' \in \{1, \dots, M\} \setminus \{m\}$, which yields $\sigma_{m'}^2/[\hat{\mathbf{\Pi}}]_{Nm'} \rightarrow \infty$. As this noise term goes to infinity the first term value for will get closer to zero for any arbitrary input. Thus, it implies that, if $\sigma_m^2/[\hat{\mathbf{\Pi}}]_{Nm} \rightarrow \infty$, the likelihood value converges to zero in whatever residual between the observation n and the GP $\mathbf{f}_{m'}$ is. *That is, if an observation is perfectly assigned to a certain output, the \mathcal{L}_{cVB} will be independent of all other outputs.* This result is crucial in verifying the validity of our model.

Tighter Bound The alternative bound \mathcal{L}_{cVB} is tighter than \mathcal{L}_{VB} due to marginalization over \mathbf{f} and \mathbf{u} instead of assigning them variational distributions. This also can be easily shown through $\mathcal{L}_{cVB} - \mathcal{L}_{VB}$ which is non-negative (King & Lawrence, 2006; Lázaro-Gredilla et al., 2012). Furthermore, \mathcal{L}_{cVB} is less sensitive to q , because \mathcal{L}_{cVB} depends on $q(\mathbf{Z})$ and $q(\mathbf{\Pi}^u)$ only, but \mathcal{L}_{VB} further depends on $q(\mathbf{f})$ and $q(\mathbf{u})$. Due to the reduced sensitivity, the convergence of \mathcal{L}_{cVB} is faster than \mathcal{L}_{VB} (King & Lawrence, 2006).